

Low-Frequency ac Measurements of the Entropy Flux Associated with the Moving Vortex Lines in a Low- κ Type-II Superconductor

Félix Vidal

Groupe de Physique des Solides, Ecole Normale Supérieure, 24 rue Lhomond, 75231 Paris, France*

(Received 27 December 1972)

We present here very detailed ac measurements of the convection heat flux \vec{J}_2^h and the induction electric field \vec{E} associated with the moving vortex lines in a low- κ type-II superconductor (Pb-4.56-at.% In). The measurements were made using an original low-frequency current-modulation method based on a second-sound technique. \vec{J}_2^h and \vec{E} have been measured as functions of the applied magnetic field H_e and the applied electric current density and frequency ν ($300 < \nu < 1200$ Hz) in the temperature range between 1.3 and 2.1 °K. The great accuracy of this ac method allows us to observe some interesting details in the $\vec{J}_2^h(H_e)$ and $\vec{E}(H_e)$ curves. In particular, $\vec{J}_2^h(H_e)$ reverses its direction at low fields ($H_e \lesssim H_{c1}$), while $\vec{E}(H_e)$ remains in the same direction in the whole of the mixed state. This reversal effect suggests that, due to the presence of nonlocal effects in our low- κ alloy ($\kappa \approx 1.25$), there are vortex lines of opposite sign in the superconductor. Furthermore, we have observed that $\vec{J}_2^h(H_e)$ vanishes only for fields larger than the upper critical field $H_{c2}(T)$. The transported entropy S_D per unit length of flux line per flux quantum computed from these measurements was found to be independent of the applied current density and frequency. In the high-field region ($H_e \gtrsim H_{c2}$) experimental values of S_D are in good agreement with the theoretical predictions of Caroli and Maki in the dirty limit. The calorimetric entropy per vortex line was obtained theoretically from the free-energy forms in the mixed state and compared with S_D .

I. INTRODUCTION

In the last years, a number of theoretical and experimental works have been reported on dynamical properties of type-II superconductors in the mixed state.^{1,2} These transport properties are accounted for in terms of a translation of the Abrikosov vortex structure: each vortex line possesses a quantum of magnetic flux ϕ_0 and an amount of entropy S_D . An applied electric current density \vec{j}_1 or a transverse local temperature gradient $\vec{\nabla}T$ exerts on a single vortex line, respectively, the Lorentz force

$$\phi_0 \vec{j}_1 \times \vec{e}_h \quad (1)$$

or the thermal force

$$-S_D \vec{\nabla}T, \quad (2)$$

where \vec{e}_h is the unit vector along the vortex line. When these forces exceed the pinning forces, the vortex lines are driven into motion and there is thus an induction electric field \vec{E} and a convection heat flux \vec{J}_2^h :

$$\vec{E} = -n\phi_0 \vec{v}_L \times \vec{e}_h, \quad (3)$$

$$\vec{J}_2^h = TnS_D \vec{v}_L, \quad (4)$$

where $n \equiv B/\phi_0$ is the vortex line density, B is the magnetic induction, T is the temperature, and \vec{v}_L is the vortex line velocity that can be determined from a phenomenological equation of movement for the vortices. For example, in the presence of an electric current density of sufficient magnitude, steady-state vortex motion of velocity \vec{v}_L obtains, where \vec{v}_L is determined by equating the net force on a vor-

tex, $\vec{f} = \vec{f}_L - \vec{f}_P$ (\vec{f}_L being the Lorentz force and \vec{f}_P the pinning force), to a viscous drag force $\eta \vec{v}_L$:

$$\eta \vec{v}_L = \vec{f}_L - \vec{f}_P \quad (5)$$

(here we have neglected the Hall effect). Equation (5) leads to a power dissipated through viscous flow: $P = \eta v_L^2$. The major contribution to P comes from Joule heating in the vortex core (one-half of P comes from dissipation in the core and one-half from dissipation arising from the return currents outside the vortex core).

A theoretical justification of this vortex-motion model has been obtained by Schmid,³ who has shown that the time-dependent Ginzburg-Landau (TDGL) equation implies that the order parameter moves with a velocity \vec{v}_L in the presence of an electric field \vec{E} . Furthermore, explicit solutions for transport coefficients have been obtained in the high-field region from the linearized TDGL equations,³⁻⁵ or by using a generalization of the linear-response theory (LRT).^{6,7} Recently, a TDGL calculation has been extended to the lower magnetic fields by Hu and Thompson,⁸ but no information is given in their paper on the thermomagnetic coefficients. Between the various transport effects in the vortex state, the thermomagnetic ones are of particular interest because they provide simultaneous information concerning E and \vec{J}_2^h , and then invaluable information concerning the transport coefficients can be obtained, particularly the entropy transported per vortex line.

In general, the simultaneous measurements of \vec{J}_2^h and \vec{E} have been performed using classical dc calorimetric methods.^{1,2,9} For example, in order

to obtain the dc Ettingshausen effect, a dc electric current is passed through a sample in the x direction (Fig. 1) and a dc magnetic field is applied in the z direction. When the electric current exceeds the critical current, vortices move in the $-y$ direction. In a thermally isolated sample, the convection heat flux J_{2y}^h produces a temperature gradient in the y direction such that there is no net heat flux across the sample. \vec{J}_2^h and \vec{E} can thus be computed from measurements of the longitudinal electric field and the transverse temperature gradient.

If the force \vec{f}_L on the vortex line is time dependent, the equation of movement for the vortices is modified by the presence of inertial and elastic forces.¹⁰ In this case the vortex-line velocity is time dependent and can be nonuniform. However, an important feature of the moving-vortex model is that, even in the case of inhomogeneities throughout the sample and nonuniform \vec{v}_L , \vec{E} and \vec{J}_2^h should again be related to the same average. If \vec{f}_L is alternative, $\vec{v}_L(t)$ must be periodic, and we can write Eqs. (3) and (4) for every Fourier component of $\vec{E}(t)$ and $\vec{J}_2^h(t)$. Then, the entropy per vortex line can be obtained from the fundamental frequency components of \vec{E} and \vec{J}_2^h .

Thus, a natural extension of the dc measurements, and an original and very sensitive test of the theory, can be obtained under ac conditions. I wish to report in this paper the results of low-frequency ac measurements of the heat flux and the electric field associated with the moving vortex lines in a low- κ type-II superconductor.

The measurements are performed using an original ac calorimetric method based on a second-sound technique: The sample is completely immersed in a superfluid helium (He II) bath; an ac electric current, $j_{1x}e^{i\omega t}$, is applied in the x direction and a dc magnetic field is applied in the z direction (Fig. 1). The ac heat flux associated with

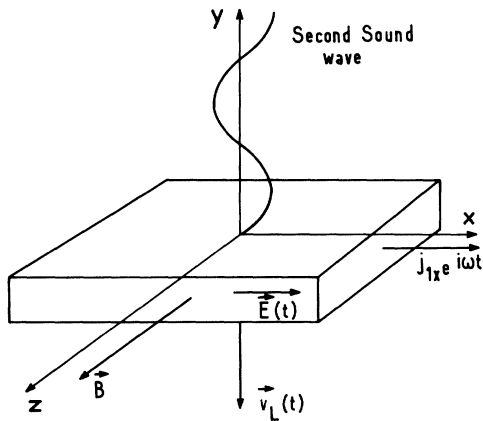


FIG. 1. Sample geometry.

the moving vortices is partially transmitted towards the He II and creates a second-sound wave that is measured with a resonant method. Essentially, the heat flux rather than $\vec{\nabla}T$ is measured. Simultaneously, the ac-induction electric field is measured using the standard ac techniques.

This ac method presents some advantages over the dc one, beyond the obvious merits of modulation. In the dc experiments, the Joule heating introduces a temperature distribution along the sample (parabolic in the ideal case), which is superimposed on the $\vec{\nabla}T$ to be measured. This circumstance limits one to small longitudinal velocities ($v_L \lesssim 10$ cm/sec). In our case it is possible to reach the linear part of the I-V characteristics (viscous flux flow) without appreciably increasing the mean slab temperature (not more than 50 m °K). Furthermore the even components (dc, 2ω , ...) of the Joule effect are well separated from the thermomagnetic effects at ω .

The essential features of this ac calorimetric technique appear in Sec. II of this paper. In Sec. III the sample parameters are given. Section IV contains the results of the measurements. The entropy transported per vortex line is computed and compared with the theoretical predictions in Sec. V. Section VI summarizes the results.

II. EXPERIMENTAL DETAILS

Measurements of the convection heat flux \vec{J}_2^h associated with the moving vortex lines were made using an original method based on a second-sound technique. A complete description of this ac technique, including calculations, test measurements, and a discussion of their advantages over conventional steady-state methods, has been reported in previous papers.¹¹⁻¹⁴ A brief outline of the essential features will be given here.

A. Experimental Method

The measurements are performed in rectangular samples completely immersed in a superfluid-helium bath. The vortex lines are created by a dc magnetic field applied in the z direction, and are driven into motion by an ac electric current, $j_{1x}e^{i\omega t}$, applied in the x direction (Fig. 1).

In the general case, the various transport current flows in the xy plane have been calculated by Maki⁵ [Eqs. (31) in Maki's paper]. Our experimental conditions impose $\vec{\nabla}T \approx 0$, $j_{1y} = 0$, and for the Pb-In alloy used here, the Hall effect can be neglected. It follows that the total heat flux \vec{J}^h and the electric field \vec{E} , given in Eqs. (31) of Maki's paper,⁵ reduce to

$$J_y^h = J_{1y}^h + nS_D T v_{Ly}, \quad (6)$$

$$E_x = -Bv_{Ly}, \quad (7)$$

where \vec{J}_1^h is the heat current in the normal state.

It must be noticed that the second term in Eq. (6) is far greater than the first term (i. e., the normal Etingshausen effect) by a factor $10^4 \sim 10^6$, and therefore J_{1y}^h can be neglected.

Moreover, as the exciting current is alternating, $v_{Ly}(t)$ is periodic (the vortices are depinned only in the current crest) and we can write Eqs. (6) and (7) for each one of the Fourier components of $E_x(t)$ and $J_y^h(t)$. The fundamental-frequency components of the total heat flux and the electric field become

$$J_y^h(\omega) \approx J_{2y}^h(\omega) = nS_D T v_{Ly}(\omega), \quad (6')$$

$$E_x(\omega) = -B v_{Ly}(\omega), \quad (7')$$

and the entropy transported per unit length of the vortex line can be directly computed from measurements of $E_x(\omega)$ and $J_y^h(\omega)$. It must be noted here that, as the Joule effect in the sample is proportional to v_L^2 , it presents only even components (dc, 2ω , ...) and it is well separated from the thermomagnetic effect at frequency ω .

As the sample is immersed in a He II bath, the heat flux $J_y^h(\omega)$ given by Eq. (6') is partially transmitted towards the He II and excites a second-sound wave at frequency ω , which is amplified in a resonant pipe terminated at one end by the sample and at the other by a carbon bolometer. The amplitude and phase of $J_y^h(\omega)$ with respect to the phase of the current $j_{1x}(\omega)$ are deduced from the second-sound bolometric signal $S(H_e)_{\omega_m}$ at the resonance, using the relation established in a previous paper¹¹:

$$S(H_e)_{\omega_m} = \left(\frac{dV}{dT} \right)_{T_0} (-1)^m Z_\infty \frac{Q}{m\pi} \alpha J_y^h(H_e)_{\omega_m},$$

where $(dV/dT)_{T_0}$ is the bolometer sensibility, H_e is the external magnetic field, ω_m is the resonance frequency for the mode m , Z_∞ is the characteristic impedance of the He II, Q is the quality factor of the second-sound cavity, and α is a complex factor depending, in particular, on the thermal skin depth δ_T and on the Kapitza resistance R_K . At the low frequencies used in our measurements ($\omega < 8000$ rad/sec), $\delta_T > \Delta y$ (the transversal dimension of our samples) and α can be approximated by¹¹

$$\alpha \approx \frac{1}{1 + 2R_K/(\Delta y/K)}, \quad (8)$$

where K is the thermal conductivity of the sample. We must notice here that expression (8) is obtained using the complementary condition: $\partial v_{Ly}/\partial y = 0$, i. e., the sample is homogeneous and the electric skin depth δ_E is much greater than Δy . In our case, $\delta_E \gg \Delta y$, if $\delta_T > \Delta y$.

B. Apparatus

The measurements were made in the apparatus shown in Fig. 2. The sample was mounted in a holder constructed of epoxy. It was designed to

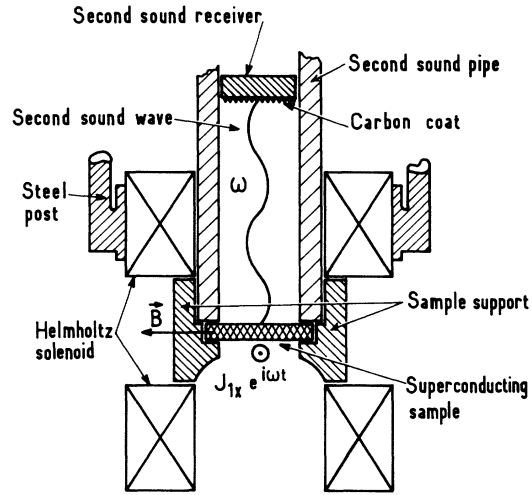


FIG. 2. Side view of apparatus.

provide maximum support against the mechanical vibrations produced by the ac current and freedom from strains produced by differences in thermal expansion. The holder is rigidly mounted in the center of a pair of Helmholtz coils that produce a magnetic field parallel to the broad face of the sample. In order to ensure the maximum surface contact between the sample and the He II bath we made, between the Helmholtz coils and in the sample support two symmetrical broad holes located opposite the broad faces of the sample. One of these holes serves as an entrance to the second-sound cavity that is situated on top of the sample. The cavity helps to maintain the sample rigidly joined to the support.

The second-sound rectangular cavity is made in Epibond and its section is $s = 12 \times 6$ mm. The other end of the resonance pipe is closed by a carbon bolometer. It is made by painting a thin coat of Aquadag-Paralac over an Epibond cork. The distance L of the bolometer to the sample is adjusted to obtain the resonance frequency desired. In order to evacuate the dc heat flux, the cavity is joined to the He II bath by two holes (1×6 mm provided at $L/2$). The cavity is designed so that it slips very easily over the sample support at room temperature but, because of the fact that the dilatation coefficient of the epoxy is greater than that of Epibond, the cavity grips the sample support at fairly low temperatures. The whole apparatus was immersed in a He II bath and was held tightly by two steel posts. The alternating current was brought down through a coaxial line that was attached to a support post. The voltage leads were mounted in such a way as to minimize inductive pickup¹³ and were attached to the outer support post.

The second-sound bolometric signal at the reso-

nance $S(H_e)_{\omega_m}$ is recorded directly in the complex plane.^{11,14} The measuring circuits are shown schematically in Fig. 3. The alternating current was supplied to the superconducting sample through an isolation and impedance adaptation transformer, by a McIntosh model-275 amplifier. The McIntosh amplifier is driven by the reference-output signal from a PAR model HR-8 phase-sensitive detector which measures the second-sound signal in phase with the transport current. Simultaneously, a second HR-8 detector, operated by the reference-output signal from the other HR-8, is used to measure the second-sound signal out of phase with the transport current. The in-phase and out-of-phase components of $S(H_e)_{\omega_m}$ are then fed into an XY recording. Measurements of $S(H_e)_{\omega_m}$ were made as functions of the magnetic field at various temperatures and electric current densities.

The measurements of the resistive voltage in and out of phase with the applied current were made as a function of the field using a classical ac method.^{10,13}

III. SAMPLE PARAMETERS

The samples used are single crystals of Pb-4.56-at.% In carefully spark cut from alloy cylinders. The single crystal was grown by the Bridgmann method and the inhomogeneity is less than 4% along 10 cm of the crystal length. This alloy was chosen because it is known to possess relatively low critical currents when properly treated, and because several detailed studies of its magnetic and thermal properties are available from previous work of other experimenters.¹⁵⁻²²

The shape of the resulting samples was that of a

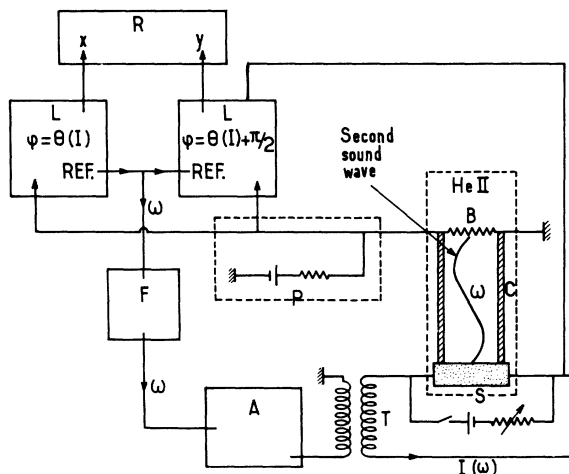


FIG. 3. Schematic block diagram of experiment. A, power amplifier 75W (MacIntosh); B, second-sound bolometer; C, second-sound cavity; F, 2ω filter; L, lock-in amplifier (HR-8); P, bolometer polarization; R, X-Y recording; S, superconducting sample; T, transformer.

rectangular slab with rounded edges; typical dimensions of the slab are $\Delta x = 25$ mm, $\Delta z = 7$ mm, $0.2 \leq \Delta y \leq 1$ mm. This geometry gives a nonzero demagnetization factor D but the shape approximates an elliptical right cylinder with a high degree of ellipticity. Thus, the values of D can be approximated by the expressions for these quantities in the case of elliptical right cylinders.²³

The relevant parameters of our samples and those quantities appearing in the calculation of S_D using the Schmid-Caroli-Maki (SCM) theory³⁻⁸ are listed in Table I. The generalized Ginzburg-Landau parameters κ_1 , κ_2 , and $\kappa(T_c)$ were derived from measurements of the magnetization as a function of the external magnetic field at constant temperature. $\kappa(T_c)$ is also determined from the normal-state resistivity ρ_N and the Gorkov-Goodman equation.²⁴ These values are in excellent agreement with the results obtained in lead-indium alloys by other experimenters.¹⁵⁻¹⁸

The ratio ξ_0/l was calculated from Gorkov's relation²⁶

$$\kappa(l) = \kappa_0 / \chi(\Lambda),$$

where κ_0 is the Ginzburg-Landau parameter in the pure limit, l is the average electronic mean free path in the normal state, ξ_0 is the coherence length, and

$$\chi(\Lambda) = \frac{8}{7\zeta(3)} \sum_{n=0}^{\infty} \frac{1}{(2n+1)^2(2n+1+\Lambda)}.$$

Here $\zeta(3) = 1.202$ and $\Lambda = 0.882(\xi_0/l)$. The value²⁷ of $\kappa_0 = 0.24$ was used in these calculations. We note that the value of ξ_0/l in Table I seems to indicate that our sample is not in the dirty limit. However, the experimental temperature dependence of κ_1 is in good agreement with the theoretical predictions of Helfand and Werthamer,²⁸ Maki,²⁹ and Eilenberger³⁰ in the case of $\xi_0/l \rightarrow \infty$. Furthermore, it is apparent that the value of κ_1 in Table I is very different from the dirty-limit value [$\kappa_1(0)/\kappa \approx 1.2$] predicted by Eilenberger and others. Their results must be modified to account for the non-BCS behavior of real superconductors.³¹ In this case, $\kappa_1(0)/\kappa \approx 1.47$ for dirty-Pb superconductors, and the experimental value of $\kappa_1(0)/\kappa$ is in excellent agreement with this value. These considerations allow us to claim that our Pb-In alloy is sufficiently "dirty" for the valid application of the dirty-limit result for S_D of the SCM theory.

In order to calculate the parameter α given by Eq. (8), it is necessary to know the thermal conductivity K of the sample and the thermal-contact resistance (Kapitza resistance) R_K between the sample and the He II.

The thermal conductivity of Pb-In alloys is at this time very well known. In our case K has been estimated from the results of Lindenfeld,¹⁹ Fox

TABLE I. Sample parameters.

Composition	a	b	c	d	e	f	g
	T_c (°K)						κ
Pb-4.56-at. % In	7.1	1.27	1.25	1.8	1.9	5	4

^a Critical temperature.

^b κ determined from measurements of the upper critical field H_{c2} at $T=4.2^\circ\text{K}$.

^c κ_1 determined from measurements of the normal-state resistivity.

^d κ_1 at $T=0$, determined from measurements of H_{c2} and H_c (the thermodynamical critical field), as $\kappa_1(T) = H_{c2}(T)/\sqrt{2} H_c(T)$.

^e κ_2 at $T=0$, determined from measurements of $(dM/dH)_{H_{c2}}$.

^f ξ_0/l calculated from Gorkov's relation.

^g Kapitza resistance at $T=2.2^\circ\text{K}$, estimated from the results of Challis and Sherlock (Ref. 32) and Cheek (Ref. 33).

et al.,²⁰ Gied *et al.*,²¹ and Gupta and Wolf.²² Since these authors did not measure at 4.56-at. % In alloy, their values of K are plotted as a function of In concentration and extrapolated to 4.56-at. % In concentration.

The Kapitza resistance of type-II superconductors has not been studied using an ac heat current. However, the measurements of Challis and Sherlock³² in Pb show that no significant difference in magnitude can be detected between the ac and dc measurements. Furthermore, some dc measurements performed by Cheeke³³ on 2- and 20-at. % In in Pb show that R_K in Pb-In alloys is comparable to R_K obtained in lead. Since R_K has not been definitely established, values of $R_K(T)$ have been estimated from the results of both Cheeke³³ and Challis and Sherlock.³² The value of R_K at $T=2.2^\circ\text{K}$ is included in Table I. Values of R_K at other temperatures are estimated using the temperature-dependent law of R_K in Pb given in Ref. 32.

IV. EXPERIMENTAL RESULTS

Typical curves for the heat flux J_{2y}^h and the electric field E_x , plotted versus the external magnetic field, are presented in Figs. 4-7. The measurements are performed at a constant temperature and with the electric current density and frequency held constant. All these experimental results are derived from measurements of the fundamental-frequency components of $J_{2y}^h(t)$ and $E_x(t)$. Moreover, all heat-flux curves in Figs. 4-7 are half the difference of the two heat fluxes obtained for opposite directions of the applied magnetic field. This averaging procedure eliminated possible spurious heat flux at the frequency ω due to the Joule effect, which did not reverse its sign upon reversal of the magnetic field. (For example, a spurious effect at the frequency ω can be created by the possible presence of the 2ω component of the electric current that, crossing with the ω component, creates a Joule effect at ω .)

Before a more detailed discussion of these re-

sults, I would like to emphasize that the general behavior of J_{2y}^h and E_x in Figs. 4(a) and 4(b) is analogous to that obtained by previous authors, using dc methods, in other type-II superconductors.^{2,9} As is expected from the vortex-motion model, J_{2y}^h appears only above a certain value H^* , when the first longitudinal voltage is just observed. This is because below H^* , flux motion does not occur since here the pinning force is larger than the Lorentz force. As the external field increases, J_{2y}^h passes through a maximum and vanishes at about the upper critical field H_{c2} .

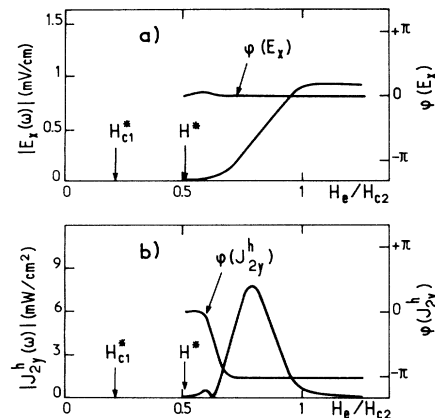


FIG. 4. (a) Amplitude and phase of the fundamental component of the longitudinal electric field versus the reduced external magnetic field $H_e/H_{c2}(T)$; $\phi(E_x)$ represents the phase of $E_x(\omega)$ with respect to the phase of the current $j_{1x}(\omega)$; $|E_x(\omega)|$ and $\phi(E_x)$ are deduced from measurements of the resistive voltage in and out of phase, with respect to the phase of the current; $H_{c1}^* \equiv H_{c1} \times (1-D)$ is the "true" lower critical field. (b) Amplitude and phase of the fundamental component of the transverse heat flux versus reduced external field; $\phi(J_{2y}^h)$ represents the phase of $J_{2y}^h(\omega)$ with respect to the phase of the applied current. The measurements in (a) and (b) were performed at $T=1.5^\circ\text{K}$ and with $j_{1x}=166 \text{ A/cm}^2$, and $\omega=2028 \text{ rad/sec}$.

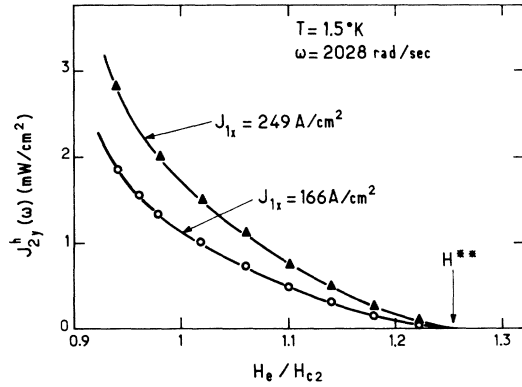


FIG. 5. Field dependence, in the critical region ($H_e \gtrsim H_{c2}$), of the fundamental component of the transverse heat flux, for two current densities.

At the low frequencies used in our experiments ($\omega < 8000$ rad/sec), a reasonable approximation of the dynamic equation of motion for the vortex is given by Eq. (5). Using Eqs. (3)–(5), the theoretical phase of $J_{2y}^h(\omega)$ and of $E_x(\omega)$ with respect to the phase of the current, $j_{1x}\sin\omega t$, can easily be estimated. E_x is in phase with $j_{1x}(\omega)$ and is in opposite phase with the Lorentz force, whereas $J_{2y}^h(\omega)$ is in opposite phase with $j_{1x}(\omega)$ and thus is in phase with the Lorentz force. Except at low fields, the phase behaviors of $J_{2y}^h(\omega)$ and $E_x(\omega)$, shown in Fig. 4, are in agreement with this phenomenological approach.

We note from Fig. 4(b) that $J_{2y}^h(\omega)$ has nonzero values above the upper critical field H_{c2} , which is determined from measurements of the magnetization curve. This effect is detailed in Fig. 5, where we show that the transversal heat flow vanishes at about a certain value $H^{**}(T) > H_{c2}(T)$. H^{**} is in-

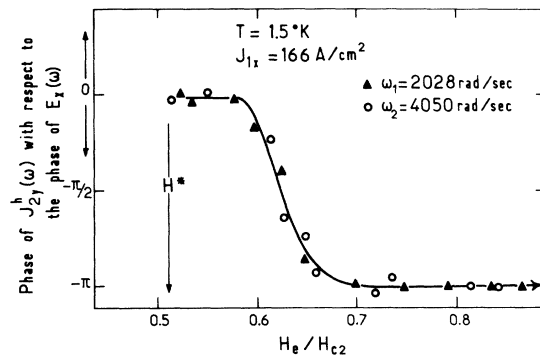


FIG. 6. Field dependence of the phase of the fundamental component of the transverse heat flux, with respect to the phase of the fundamental component of the longitudinal electric field. The frequencies ω_1 and ω_2 of the applied current correspond to the frequencies of the two first resonant modes of the second-sound cavity.

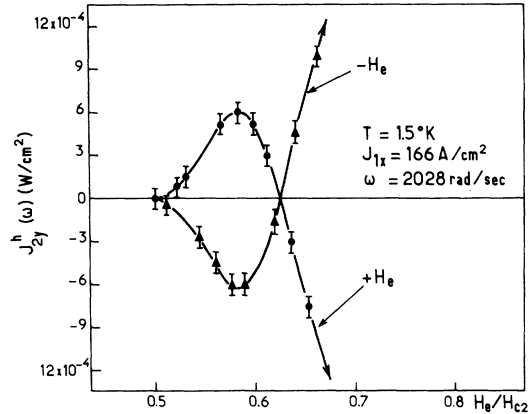


FIG. 7. Field dependence of the amplitude of the fundamental component of the transverse heat flux, in the low-field region. The two symmetric curves are obtained by inversion of the external magnetic field.

dependent of the frequency and density of the applied current. The appearance of a small heat flow above H_{c2} had been noticed first by Fiory and Serin.³⁴ These authors found that the Ettingshausen coefficient of pure niobium changed its sign at H_{c2} , attaining a small value above H_{c2} . Later, an analogous effect was observed by Huebener and Seher³⁵ in the Nernst coefficient. These results in a pure superconductor³⁶ are accounted for in terms of a contribution of the normal heat flow \vec{J}_1^h to the total heat flow \vec{J}^h given by Eq. (6). This explanation cannot be applied in our case, because \vec{J}_1^h is a negligible effect in dirty superconductors. Furthermore, the striking feature of the data in Fig. 5 is the decreasing of the heat flow above H_{c2} when H_e increases, while J_1^h should be proportional to H_e .

Moreover, in order to test the role of the surface superconductivity on the heat flux that we observe below H_{c2} , we have made some measurements in the same alloy, but coating the sample with a layer of normal material (gold). In this manner the surface sheath is destroyed. There are some difficulties in making a quantitative comparison between both experimental situations, because other properties of the sample, particularly the Kapitza resistance, are also modified by the presence of the Au layer. However, and in spite of some variations of both J_y^h and H^{**} , we observe that J_y^h still exists below H_{c2} when the surface superconductivity is destroyed. Consequently, the effect shown in Fig. 5 must be considered as a new experimental feature which shows that in the critical region ($H_e \gtrsim H_{c2}$), the thermomagnetic effects in type-II superconductors cannot be explained in terms of a simple vortex moving model.

Note from Fig. 4(b) that at low fields the phase of $J_{2y}^h(\omega)$, with respect to the phase of $j_{1x}(\omega)$, ro-

tates to give a small peak at opposite phase to the Lorentz force. At the same time the phase behavior of $E_x(\omega)$ is slightly different, its in-phase component remains positive, and we observe a positive peak in the $\frac{1}{2}\pi$ component ($\sim 5 \mu\text{V}/\text{cm}$). This effect is independent of the density and frequency of the current.

The striking but well-established feature of this heat-flux behavior is that, at low fields when the current just begins to depin the vortices, the phase of $J_{2y}^h(\omega)$ with respect to the phase of $E_x(\omega)$ changes sign. This effect, noted in a previous paper,¹² is detailed in Fig. 6, where the phase of $J_{2y}^h(\omega)$ with respect to the phase of $E_x(\omega)$ is plotted versus the external field. The amplitude of J_{2y}^h in this field range is shown in Fig. 7. The two curves of J_{2y}^h are obtained for opposite directions of the applied magnetic field. Since the data in Fig. 7 contain only the heat flux which reversed its sign upon reversal of the magnetic field, any contribution of the Joule effect to the heat flux is eliminated.

A sign reversal between J_{2y}^h and \vec{E} still has not been observed using dc techniques,³⁷ and is difficult to explain by the classical models of vortex motion. We have performed preliminary analogous measurements in a high- κ Pb-In alloy ($\kappa \approx 7$) and the reversal effect is not observed. This suggests that the possible presence of nonlocal effects in the low- κ alloy, where the reversal effect is observed, must drastically modify the magnetic flux distribution into the sample, and thus the flux flow can be modified.

In fact, it is well known that the appearance of a nonlocal relation between electric current and magnetic field leads to a change in the sign of the field penetrating into the superconductor.³⁸ Recent calculations³⁹ show that there is still a sign reversal of the magnetic field in type-II superconductors with a Ginzburg-Landau parameter, $\kappa \leq 1.6$. A model of an isolated vortex line, when the nonlocal relation between current and vector potential are taken into account, has been suggested by Jacobs.⁴⁰ Recently, Dichtel,⁴¹ using an approximation of the BCS kernel, has given an analytic expression of the magnetic field of a single flux line at $T=0$ for low- κ type-II superconductors. This calculation has been extended to the whole temperature range by Brand.⁴² According to these models for an isolated vortex line, close to the axis of the vortex the local magnetic field \vec{h} and the superfluid velocity \vec{v}_s are the sign of the applied magnetic field, whereas far from the axis, \vec{h} and \vec{v}_s would be the opposite sign. In the vortex lattice, field reversal is expected to occur only for a large lattice constant. In our measurements we observe a reversal-heat-flux effect for magnetic inductions $B \approx 1000$ G, thus for an intervortex distance $d = [2\phi_0/B\sqrt{3}]^{1/2} \approx 1500$ Å. As in the Pb-In alloy used here the penetration depth

is $\lambda \approx 500$ Å and we have $d/\lambda \approx 3$.

It is possible now to explain the sign reversal between \vec{J}_2^h and \vec{E} in terms of the vortex-line motion, if we assume that, owing to the nonlocal effects, there are in the sample vortex lines of opposite sign (with magnetic flux $\phi_0\vec{e}_h$ and $-\phi_0\vec{e}_h$ and respective densities such that the total magnetic flux is conserved). If the vortex line is reversed, the Lorentz force [Eq. (1)] is reversed, and thus \vec{v}_L changes sign. Then, the induction electric field given by Eq. (3) keeps the same sign, but the convection heat flux \vec{J}_2^h given by Eq. (4) changes sign. Moreover, owing to the sign-reversal effect, the interaction forces between the vortex lines must be drastically modified. In fact, the experimental observations obtained at low magnetic fields from decoration techniques show the existence of mixtures of Shubnikov and Meissner phases in critical- κ type-II superconductors, which demonstrates the existence of attractive forces between the vortices beside the repelling forces.^{43,44} The sign reversal between \vec{J}_2^h and \vec{E} at low fields would thus be explained assuming that the negative vortex lines move before the normal vortices,⁴⁵ and that their density decreases as the total vortex density increases.

We would like to conclude this discussion with an additional remark. The heat-flux-reversal effect appears when the transverse current just begins to depin the vortices, i. e., when the current starts to penetrate into the superconductor. Then, we cannot exclude the presence of surface effects. However, it should be emphasized that we can obtain a simple picture of the reversal effect in terms of the moving-vortex-line model making the assumption that, at low fields ($H_e \geq H_{c1}$), there are opposite vortex lines in the sample. To verify our conjecture, further experiments would, however, be desirable to test the κ and high-temperature dependence of the sign-reversal effect. On the theoretical side, the theory of an isolated vortex line, when the nonlocal relation between field and current is taken into account, should be extended to the vortex-lattice case.

V. ENTROPY TRANSPORTED PER VORTEX LINE

A. Experimental Results

Figure 8 shows the entropy transported per meter of flux line per flux quantum as a function of the magnetic field at $T = 1.38$ °K. The results at other temperatures are similar. The values of S_D were derived from the data of $J_{2y}^h(\omega)$ and $E_x(\omega)$ using the relation obtained from Eqs. (6) and (7),

$$S_D = \frac{\phi_0}{T} \frac{|J_{2y}^h(\omega)|}{|E_x(\omega)|}. \quad (9)$$

Before discussing these results let us emphasize

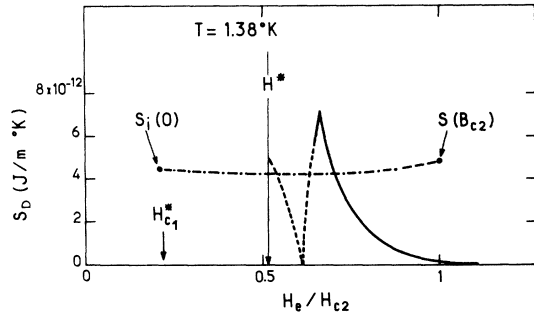


FIG. 8. Magnetic field dependence of S_D , the entropy transported per unit length of vortex line. The dashed part of the S_D curve corresponds to the field region where the phase of $J_{2y}^h(\omega)$ changes sign. The dot-dash curve is S_i , the theoretical estimate incremental entropy per vortex line. S_i is calculated from the expressions of the free-energy density in the mixed state, as explained in the text.

that (i) we have verified that S_D is independent of the vortex velocity, i. e., $J_{2y}^h(\omega)$ is proportional to $E_x(\omega)$ at a given field and temperature. To prove this, $J_{2y}^h(\omega)$ and $E_x(\omega)$ were measured as a function of the current density. Figure 9 shows $J_{2y}^h(\omega)$ versus the vortex line velocity, and the expected linearity is evident. Analogous results in the dc case have been obtained previously by Otter and Solomon.^{9,46} (ii) We have found that S_D is almost independent of the frequency ω of the electric current, for $\omega < 8000$ rad/sec (Fig. 10). To obtain S_D vs ω , $J_{2y}^h(\omega)$ and $E_x(\omega)$ were measured at the frequencies corresponding to the four first resonant modes of the second-sound cavity. Since $E_x(\omega)$ is almost frequency independent, this result proves that our low-frequency approximation to calculate the coefficient α in Eq. (8) is a correct treatment.

At high fields, the general behavior of S_D vs field shown in Fig. 8 is in agreement with that obtained from dc measurements by previous authors in other type-II superconductors.^{2,9} S_D starts at about H_{c2} with a negative slope and depends linearly on H_e .

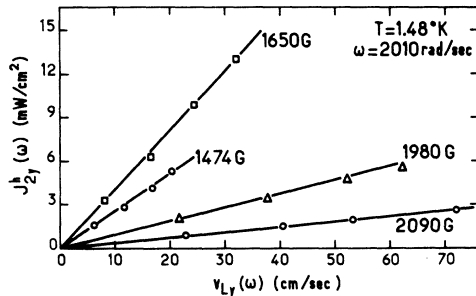


FIG. 9. Transverse heat flux versus vortex line velocity. v_L is obtained using Eq. (7').

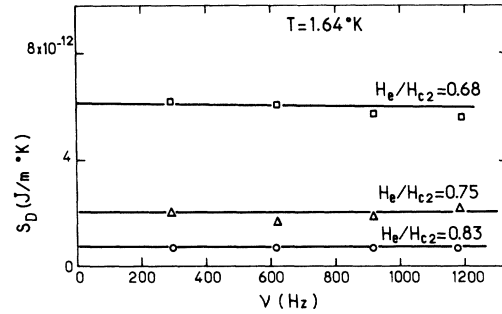


FIG. 10. Entropy transported per vortex line versus applied current frequency for different magnetic fields.

When H_e decreases the negative slope of S_D increases very rapidly and we observe a maximum around 1400 Oe, followed by a zero minimum at low field. A similar low-field dip has been observed by Otter and Solomon near H_{c1} in a Nb-Mo alloy.⁴⁷ These authors suggest that the low-field dip is due to trapped vortices existing below H_{c1} . In our case, the low-field region of S_D (the dashed part of the S_D curve in Fig. 8) corresponds to the field region where the phase of $J_{2y}^h(\omega)$, with respect to the phase of $E_x(\omega)$, changes sign. If the reversal effect of J_2^h is due to a changing sign of the local magnetic field of the vortices, the heat flux in this region should be the difference between two opposite heat fluxes corresponding to the opposite vortices. Then, Eq. (9) cannot be applied to compute the entropy per vortex line in this low-field region.

B. Comparison with Theory

1. High-Field Region

In the high-field region ($H_e \lesssim H_{c2}$) explicit solutions for the transport coefficients have been obtained using two different theoretical approaches: (i) a generalization of linear response theory (LRT) to include the effects of dynamical fluctuations of the order parameter,^{6,7} and (ii) methods which make use of the TDGL equation.³⁻⁵ Such microscopic calculations are based on the fact that, close to H_{c2} , the order parameter Δ is small and proportional to $(H_{c2} - H_e)^{1/2}$. Physical quantities will be expanded with respect to Δ up to its second order. Recently, Houghton and Maki⁸ have shown the consistency of both TDGL and LRT methods. In particular, these authors give an explicit calculation of the Ettingshausen coefficient in LRT, which is found to agree with the earlier TDGL calculation.⁵

For the dirty-limit situation, the heat current due to the moving order parameter is given by^{5,8}

$$J_{2y}^h = ME_x L_D(T) \quad (10)$$

and

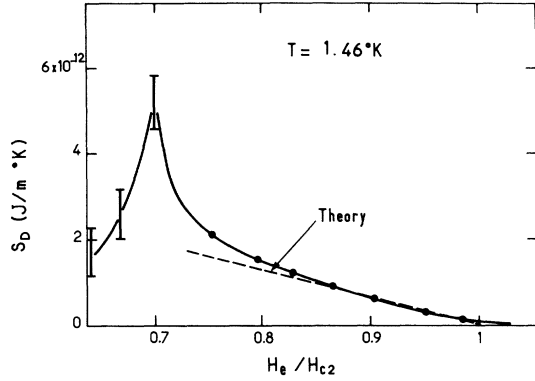


FIG. 11. Field dependence of S_D in the high-field region [$H_e \lesssim H_{c2}(T)$]. The dashed curve is calculated from Eq. (12).

$$L_D = 1 + \rho \frac{\Psi^{(2)}(\frac{1}{2} + \rho)}{\Psi^{(1)}(\frac{1}{2} + \rho)},$$

where ρ is determined by

$$-\ln(T/T_c) = \Psi(\frac{1}{2} + \rho) - \Psi(\frac{1}{2}).$$

Here $\Psi(Z)$, $\Psi^{(1)}(Z)$, etc., are the digamma function and its higher-order derivatives. From Eqs. (3), (4), and (10), the entropy carried by a single vortex line is easily found:

$$S_D = -(\phi_0/T)ML_D(T). \quad (11)$$

Cape and Zimmerman⁴⁸ have earlier considered the effects of the nonzero demagnetization factor D upon the magnetization of ellipsoidal superconductors. Their result for the external field H_e parallel to a principal axis is expressed as

$$M = [H_e - H_{c2}(T)] / \{1.16[2\kappa_2^2(T) - 1] + D\}.$$

Combining this result with that of the SCM theory [Eq. (11)], S_D can be expressed as

$$S_D = \frac{\phi_0}{T} \frac{H_{c2} - H_e}{1.16[2\kappa_2^2 - 1] + D} L_D. \quad (12)$$

This expression of S_D has the usual validity range of the Ginzburg-Landau theory. [$H_{c2}(T) - H_e$] $\ll H_{c2}(0)$. This is because the so-called anomalous term⁶ does not contribute to the Ettingshausen effect.⁷

The field dependence of S_D at $T/T_c = 0.2$ is detailed in Fig. 11. Also presented in the figure is the theoretical curve using Eq. (12). The theoretical values of S_D were calculated using the data of Table I and $H_{c2} = 2150$ Oe and $\kappa_2 = 1.8$ at $T/T_c = 0.2$. In the high-field range ($H_e \gtrsim 0.8 H_{c2}$), the agreement between the experimental result and the theoretical one is quite excellent.

In order to make a direct comparison with experimental data in the range $H_e \rightarrow H_{c2}$, it is useful

to calculate the quantity

$$S' \equiv \left(\frac{\partial S_D}{\partial H_e} \right)_{H_e = H_{c2}} = - \frac{\phi_0}{T_c} \frac{L_D / (T/T_c)}{1.16(2\kappa_2^2 - 1) + D}. \quad (13)$$

The temperature dependence of S' is shown in Fig. 12. The curve expresses results of Eq. (13). The temperature dependence of $\kappa_2(T)$ used in Eq. (13) has been determined from our experimental results and also from the results of both Farrell *et al.*¹⁵ and Dubeck *et al.*¹⁷ As one can see in Fig. 12, the theory comes close to the experiment.

2. Fields below H_{c2}

Below $H_{c2}(T)$, it is not possible to treat the effects of the energy gap as a perturbation. Thus, the theoretical approaches previously indicated are not applicable and actually there is no microscopic theory of the transport effects in this field region. However, for $H_e \ll H_{c2}$, the TDGL equation can be linearized in the regions near, and far from, the vortex core, and explicit features of the solution can be obtained. Recently, Hu and Thompson,⁸ using a set of approximate TDGL equations introduced by Schmid,³ have obtained the field and charge distributions around an isolated vortex line moving in a transport current. In their work, Hu and Thompson have calculated the initial slope of the flux-flow resistance, but no information is given on the thermomagnetic coefficients.

Many phenomenological theories, based on the analogy between the mixed state in type-II superconductors and the similar one in superfluid helium, have been proposed to account for the dissipative phenomena.¹ These theories deal with the low-field region ($H_e \gtrsim H_{c1}$), where the distance d between vortex lines is much larger than the coherence distance ξ . These models assumed that each vortex line carries an amount of entropy S_D corre-

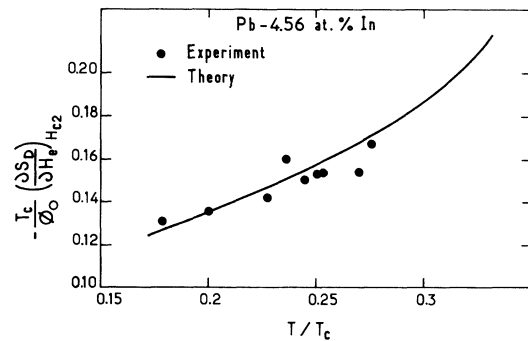


FIG. 12. Temperature dependence of the derivative of the transport entropy (multiplied by T_c/ϕ_0) with respect to magnetic field near H_{c2} . The curve is calculated from Eq. (13) in terms of $\kappa_2(T)$ obtained from magnetization measurements.

sponding to the excitations which are trapped in its core. S_D is expected to be smaller, or equal when $B \rightarrow 0$ (i. e., when $d \gg \xi$), than S_i , the equilibrium entropy per vortex line. S_i is associated with the reversible creation or destruction of a vortex line and includes all (local and nonlocal) excitations associated with the vortex line.⁹ The equilibrium entropy per vortex line can be defined by the relation⁴⁹

$$dS = c \frac{dT}{T} + S_i \frac{dB}{\phi_0},$$

where $S(B, T)$ is the total entropy density and c the specific heat. In terms of the free-energy density ($dF = -SdT + H_e dB$), S_i can be expressed as

$$S_i = -\phi_0 \frac{\partial^2 F}{\partial B \partial T}.$$

The equilibrium entropy per vortex line is consequently a thermodynamic coefficient of the same kind as the specific heat c and must exhibit a discontinuity at $H_{c2}(T)$ (second-order transition). Theoretical expressions of $S_i(B, T)$ have been obtained from the free-energy forms in high- κ type-II superconductors.⁴⁹ Some of these expressions of S_i are still valid in low- κ type-II superconductors and can be applied to calculate S_i in our Pb-In alloy. Close to H_{c1} , we have⁴⁹

$$\begin{aligned} S_i(0, T) &= -\phi_0 \frac{dH_{c1}(T)}{dT} \\ &= \frac{\sqrt{2} \phi_0 H_c(0)}{T_c} \frac{\ln \kappa_3(T)}{\kappa_3(T)} \\ &\quad \times \left[(T/T_c) - \frac{1 - (T/T_c)}{2 \ln \kappa_3(T)} [1 - \ln \kappa_3(T)] \kappa_3'(T) \right], \end{aligned} \quad (14)$$

and at $H_{c2}(T)$ we have⁴⁹

$$\begin{aligned} S_i(B_{c2}, T) &= S_i(0, T_c) \frac{\kappa_1(T) \kappa / \ln \kappa}{1.16(2\kappa^2 - 1) + D} \\ &\quad \times [2(T/T_c) - [1 - (T/T_c)^2] \kappa_1'(T)], \end{aligned} \quad (15)$$

where $\kappa_1'(T) \equiv T_c(1/\kappa_1)(d\kappa_1/dT)$. From the Eqs. (14) and (15) we have computed S_i in our Pb-In alloy. Results of these calculations at $T = 1.38$ °K are shown in Fig. 8. Similar results are obtained at other temperatures. At intermediate field, S_i has been estimated using the same approaches as in the case of high- κ superconductors.⁴⁹ A comparison between S_i and S_D at low fields is very hazardous because in our case we believe that, owing to the reversal effect, S_D is not well established in this field region. At intermediate fields, where S_D is well established, we observe that $S_D > S_i$. It is possible that the approaches used to estimate S_i in this field range are not valid in low- κ supercon-

ductors. However, we have shown previously⁴⁹ that $(\partial S_i / \partial B_e)_{B_{c1}} < 0$, and to the second order in $(B_e - B_{c2})$, $(\partial S_i / \partial B_e)_{B_{c2}} > 0$. These results are valid whatever the value of κ . We believe that in the case of our Pb-In alloy, the previously indicated result near H_{c2} is not affected by the next-order terms in the expansion in powers of $(B_{c2} - B_e)$ of the free energy,⁵⁰ and a minimum of S_i must be expected at intermediate fields. Thus, the uncertainties in S_i and S_D at intermediate fields are much too small to account for the fact that $S_i < S_D$ observed in Fig. 8, and they must be considered real. We must notice here that similar discrepancies between S_i and S_D have been observed previously by Solomon and Otter^{9,47} in high- κ Pb-In and Nb-Mo alloys.

I would like to conclude this comparison between S_i and S_D by emphasizing that their discrepancies must be interpreted as simply a consequence of the fact that phenomenological theories based on the two-fluid model can only give a poor approximation of the transport effects in type-II superconductors. This is probably due to the fact that, while in He II the superfluid component is made of Bosons, in a superconductor the superfluid is made of electron pairs, which respond differently to perturbations having different time-reversal symmetries. This situation, owing to the internal structure of the electron pairs, cannot be described consistently by a two-fluid model. Moreover, the electric and heat-current expressions obtained using the phenomenological Ginzburg-Landau equations are in disagreement with the results obtained using the microscopic theories.⁵¹

VI. CONCLUSIONS

We have used an original low-frequency current-modulation method to investigate the convection heat flux \vec{J}_2^h and the induction electric field \vec{E} associated with the moving vortex lines in a low- κ type-II superconductor. \vec{J}_2^h and \vec{E} have been measured as functions of the applied magnetic field H_e , and the frequency and amplitude of the applied electric current, in the temperature range between 1.3 and 2.1 °K.

The magnetic field dependence of \vec{J}_2^h and \vec{E} shows a general behavior similar to that obtained by previous authors, using dc methods, in other type-II superconductors. However, the great accuracy of this ac method (we can measure heat flux of less than 10^{-5} W/cm²) allows us to observe some interesting details on the $\vec{J}_2^h(H_e)$ and the $\vec{E}(H_e)$ curves. In particular, the field dependence of \vec{J}_2^h shows a behavior changing sign at low fields ($H_e \gtrsim H_{c1}$), while $\vec{E}(H_e)$ remains positive. As this effect is found to be independent of the applied current frequency (2000 $< \omega < 8000$ rad/sec), one is led, by a continuity argument, to the conclusion that the effect must

exist in the steady-state case. However, in the field range for which the reversal effect occurs, \bar{J}_2^h is perhaps too small to make the observation possible in the dc case (typically, $J_{2y}^h \approx 10^{-5}$ W/cm² in this field range and with $v_L \approx 0.1$ cm/sec, and in an isolated sample, we would have $\nabla_y T \approx 5 \times 10^{-4}$ °K/cm).

To explain this reversal effect in terms of the vortex-line motion, we have suggested that, owing to the existence of nonlocal effects in our low- κ type-II superconductor ($\kappa \approx 1.25$), there are opposite vortex lines in the sample at low fields.⁵² To verify our conjecture further experiments would, however, be desirable to test the κ and high-temperature dependence of the sign-reversal effect. On the theoretical side, the theory of an isolated vortex line, when the nonlocal relation between field and current is taken into account, should be extended to the vortex-lattice case.

On the other hand, we have observed that $J_y^h(H_e)$ vanishes only for fields larger than $H_{c2}(T)$. This heat flux cannot be attributed to the normal Ettingshausen effect. Moreover, it is difficult to explain this heat flux in terms of moving vortex lines, because in this field region the mean bulk magnetization becomes negligible and the material is usually regarded as normal. However, as is well known, the dynamical properties of type-II superconductors in the vicinity of the transition point can be strongly modified because of the thermodynamical

fluctuations of the order parameter.^{6,53} The occurrence of these critical fluctuation effects in the Ettingshausen heat flux may provide an explanation for the observed effect.

From these measurements the transport entropy S_D per unit length per flux quantum has been computed and compared to the existing theories. In the high-field region ($H_e \lesssim H_{c2}$), S_D is in excellent agreement with the theoretical predictions of Caroli and Maki in the dirty limit. The calorimetric entropy per vortex line, S_l , has been estimated theoretically from the free-energy forms in the mixed state. We found that in the intermediate field region ($H_{c1} < H_e < H_{c2}$), $S_D > S_l$. This result would show that phenomenological theories, based on the two-fluid model, are not valid to explain the thermomagnetic effects in type-II superconductors. More meaningful comparison will not be possible until the microscopic theory is extended to a larger region of validity.

ACKNOWLEDGMENTS

I am grateful for the helpful remarks of Professor J. Bok and Dr. C. Caroli. The author wishes to express his gratitude to Professor M. Le Ray and Professor Y. Simon, who suggested this experiment and for their constant help. A series of useful conversations with Dr. M. Francois and Dr. D. Lhuillier are gratefully acknowledged.

*Laboratoire associé au Centre National de la Recherche Scientifique.

¹For a comprehensive review, see, for example, Y. B. Kim and M. J. Stephen, in *Treatise on Superconductivity*, edited by R. D. Parks (Marcel Dekker, New York, 1969).

²For a recent exposition of experiments, see the series of articles on the thermomagnetic effects in type-II superconductors [Physica (Utr.) 55 (1971)].

³A. Schmid, Phys. Kondens. Mater. 5, 302 (1966).

⁴C. Caroli and K. Maki, Phys. Rev. 164, 591 (1967). The TDGL equation used in this paper is only correct in the vicinity of the transition temperature, as has been shown by H. Ebisawa and H. Takayama [Prog. Theor. Phys. 42, 1481 (1969)]. However, as has been pointed out by R. S. Thompson [Phys. Rev. B 3, 1617 (1971)], the error is compensated for in the calculation of the electric current, so that contribution to the current calculated in Ref. 4 is correct (see also Ref. 7). In addition, in this paper Caroli and Maki use thermodynamical arguments to claim that, as they found from TDGL calculations, the entropy S_D transported by a vortex line must vanish at H_{c2} . However, thermodynamical considerations are not valid in this case, which is a typical nonequilibrium situation. In fact, an easy calculation shows that the equilibrium entropy S_l per vortex line, that can be obtained as a second-order derivative of the free energy density expression at H_{c2} , must exhibit a discontinuity at $H_{c2}(T)$ (as it should be at a second-order transition) (see also Sec. V of this paper).

⁵K. Maki, J. Low Temp. Phys. 1, 45 (1969); Prog. Theor. Phys. 41, 902 (1969). The calculations in Ref. 4 lead to the fact that the entropy S_D carried by a vortex diverges at $T \rightarrow 0$ °K. In order to eliminate this difficulty, in these papers Maki has taken

into account the energy flow due to the change of the magnetization [see also, K. Maki, Phys. Rev. Lett. 21, 1755 (1968)]. But then, as has been shown by H. Takayama and H. Ebisawa [Prog. Theor. Phys. 44, 1450 (1970)], the Onsager's reciprocal theorem is violated. In order to get rid of this new difficulty, Takayama and Ebisawa suggest that it is necessary to add, to the total electric current, some additional current, the nature of which is quite unknown at present. This problem is directly connected with the definition of the heat-current operator and, accordingly, with the exact microscopic treatment of the temperature gradient [see, for instance, R. S. Thompson and C. R. Hu, Phys. Rev. Lett. 27, 1352 (1971), and Ref. 7].

⁶C. Caroli and K. Maki, Phys. Rev. 159, 306 (1967); Phys. Rev. 159, 316 (1967); R. S. Thompson, Phys. Rev. B 1, 327 (1970); Phys. Rev. B 2, 1433 (1970).

⁷A. Hughton and K. Maki, Phys. Rev. B 3, 1625 (1971).

⁸C. R. Hu and R. S. Thompson, Phys. Rev. B 6, 110 (1972).

⁹P. R. Solomon and F. A. Otter, Jr., Phys. Rev. 164, 608 (1967).

¹⁰See, for example, P. P. Meincke and W. A. Reed, Phys. Rev. 179, 463 (1969).

¹¹F. Vidal, Y. Simon, M. Le Ray, and P. Thorel, Rev. Phys. Appl. 4, 50 (1969).

¹²Y. Simon and F. Vidal, Phys. Lett. 30A, 109 (1969).

¹³F. Vidal, thèse de 3ème cycle (Université de Paris, 1970) (unpublished).

¹⁴F. Vidal and Y. Simon, Phys. Lett. A 36, 165 (1971).

¹⁵D. E. Farrell, B. S. Chandrasekhar, and H. V. Culbert, Phys. Rev. 177, 694 (1969).

¹⁶H. V. Culbert, D. E. Farrell, and B. S. Chandrasekhar, Phys. Rev. B 3, 794 (1971).

- ¹⁷L. W. Dubeck, D. R. Aston, and F. Rothwarf, Phys. Rev. B1, 1593 (1970).
- ¹⁸E. Trojnar, Physica (Utr.) **45**, 357 (1969).
- ¹⁹P. Lindenfeld, Phys. Rev. Lett. **6**, 613 (1961).
- ²⁰G. T. Fox, M. W. Wolfmeyer, and S. R. Dillinger, Phys. Rev. **177**, 756 (1969).
- ²¹R. E. Giedd and C. A. Reynolds, Phys. Rev. B **6**, 3533 (1970).
- ²²A. K. Gupta and S. Wolf, Phys. Rev. B **6**, 2595 (1972).
- ²³W. F. Brown, Jr., *Magnetostatic Principles in Ferromagnetism* (North-Holland, Amsterdam, 1962), Appendix, p. 187.
- ²⁴B. B. Goodman, IBM J. Res. Dev. **6**, 62 (1962).
- ²⁵E. Helfand and N. R. Werthamer, Phys. Rev. **147**, 288 (1966).
- ²⁶L. P. Gorkov, Zh. Eksp. Teor. Fiz. **37**, 1407 (1959) [Sov. Phys.-JETP **10**, 998 (1960)].
- ²⁷F. W. Smith, A. Bartoff, and M. Cardona, Phys. Kondens. Mater. **12**, 145 (1970).
- ²⁸E. Helfand and N. R. Werthamer, Phys. Rev. **147**, 288 (1966).
- ²⁹K. Maki, Physics (N.Y.) **1**, 21 (1964).
- ³⁰E. Eilenberger, Phys. Rev. **153**, 584 (1967).
- ³¹G. Cody, in Proceedings of the 1968 Summer Study of Superconducting Devices Accelerators, Brookhaven National Laboratory, Part II, p. 406 (unpublished).
- ³²L. S. Challis and R. A. Sherlock, J. Phys. C **3**, 1193 (1970).
- ³³J. D. N. Cheeke, Cryogenics **10**, 463 (1970).
- ³⁴A. T. Fiory and B. Serin, Phys. Rev. Lett. **19**, 227 (1967).
- ³⁵R. P. Huebener and A. Seher, Phys. Rev. **181**, 701 (1969).
- ³⁶Recently, Otter and de Lange [F. A. Otter, Jr. and O. L. de Lange, Bull. Am. Phys. Soc. **18**, 329 (1971)] observed in a dirty superconductor a Nernst voltage at fields greater than H_{c2} , but they believe this to be a consequence of vortex motion at the cold end of the sample where $H_e < H_{c2}$.
- ³⁷Recently, Hering and Cruceanu [E. Hering and E. Cruceanu, Phys. Lett. A **38**, 431 (1972)] observed a sign reversal of the Hall angle in the mixed state. However, these authors do not report here simultaneous thermal measurements.
- ³⁸A. B. Pippard, Proc. Phys. Soc. Lond. A **216**, 547 (1953).
- ³⁹J. Halbritter, Z. Phys. **243**, 201 (1971).
- ⁴⁰A. E. Jacobs, Phys. Rev. B **4**, 3029 (1971).
- ⁴¹K. Dichtel, Phys. Lett. A **35**, 285 (1971).
- ⁴²E. H. Brand, Phys. Lett. A **39**, 193 (1972).
- ⁴³N. V. Sarma, Philos. Mag. **18**, 171 (1968).
- ⁴⁴U. Krägeloh, Phys. Status Solidi **42**, 559 (1970).
- ⁴⁵Recently, Kim [Y. B. Kim, in *Proceedings of the Twelfth International Conference on Low Temperature Physics, Kyoto, 1970*, edited by Eizo Kanda (Keigaku, Tokyo, 1971), p. 231] suggested the possibility that in the flux flow, only part of the vortex lines moves, and the rest remain stationary. However, at high fields it is reasonable to assume that all vortex lines move uniformly in one direction. This is because, in the *absence of field reversal effects*, the rigidity of the vortex lattice due to the existence of strong repelling forces between the vortex lines (that can be easily estimated from the expression of the interaction free energy F_I between vortex lines, as $-\nabla^2 F_I$) is sufficient to overcome the local pinning forces [Y. Simon, *thèse* (Université de Paris, 1969) (unpublished)]. For example, we can compare here the repelling and the pinning forces in the case of the Pb-In alloy used here. The repelling forces on a vortex line displaced $d\vec{r}$ from the equilibrium position \vec{r} , can be expressed in the form $\vec{j} \times \phi_0 \vec{L}_0$, where j is the current created at $\vec{r} + d\vec{r}$ by the entire vortex lattice. For simplicity, in determining j we consider here only the contribution of the nearest vortex line situated at the distance d . In this case F_I can be approximated by [see, for example, P. G. de Gennes, *Superconductivity of Metals and Alloys* (Benjamin, New York, 1966)]: $F_{12} = (\phi_0^2/2\pi\mu_0\lambda^2)K_0(r/\lambda)$, where K_0 is the zero-order Bessel function. Then $j = (\phi_0/\pi\mu_0\gamma^4)K''(d/\lambda)$ and for $B = 1300$ G and $T = 1.5^\circ\text{K}$ ($d/\lambda \approx 3$), we found: $j \approx 200$ A/mm² for Angstrom of separation from the equilibrium position. These values of j should be compared to the critical current density j_c (defined by the appearance of a longitudinal voltage), due to the presence of the pinning forces, that, in this case is $j_c \lesssim 15$ Å/cm².
- ⁴⁶F. A. Otter, Jr. and P. R. Solomon, Phys. Rev. Lett. **16**, 308 (1966).
- ⁴⁷F. A. Otter, Jr. and P. R. Solomon, *Proceedings of the Eleventh International Conference on Low Temperature Physics*, edited by J. F. Allen, D. M. Finlayson, and D. M. MacCall (University of St. Andrews Printing Department, St. Andrews, Scotland, 1969), p. 841.
- ⁴⁸J. A. Cape and J. M. Zimmerman, Phys. Rev. **157**, 416 (1967).
- ⁴⁹F. Vidal, Solid State Commun. **8**, 2147 (1970).
- ⁵⁰O. L. de Lange and F. A. Otter, Jr., Solid State Commun. **9**, 1929 (1971).
- ⁵¹C. Caroli, Comptes-Rendus du 5ème Colloque Sovie-Français de Bacouriani sur la Superfluidité, Tbilissi, 1968, Vol. I. p. 5 (unpublished); and private communication.
- ⁵²Very recently, Le Ray *et al.* [M. Le Ray, J. P. Deroyon, M. J. Deroyon, M. François, and F. Vidal, in the Proceedings of the Thirteenth International Conference on Low Temperature Physics, Boulder, Colo., 1972 (unpublished)] have suggested the existence of opposite vortex lines in rotating He II due to a modification of the vortex lattice by a superimposed transverse heat flow.
- ⁵³See, for example, the article of R. E. Glover, III, Ref. 2, p. 3.